

ALMA MATER STUDIORUM – UNIVERSITÀ DI BOLOGNA

SCHOOL OF SCIENCE

Laurea Magistrale in Analisi e Gestione dell'Ambiente
Curriculum in Water and Coastal Management

**COASTAL FLOODING RISK ASSESSMENT AT GARACHICO –
CANARY ISLANDS**

Master thesis in: Integrated Coastal Zone Management

Presented by: Jose Eduardo Carneiro Barros

Coordinator: Elena Fabbri

Supervisor: Juan Garzon Hervas

Co-supervisor: Javier Lopez Lara
Co-supervisor: Theocharis Plomaritis

List of Figures

| | |
|---|----|
| Figure 1: Location map of Garachico, Canary Islands, with a satellite view of the study site. | 14 |
| Figure 2: Wind rose representation for the wave climate from 1985 to 2005, showing the main incident wave directions as well as the significant wave height associated with it. | 15 |
| Figure 3: Cross-section representation of the three profiles as well as a 3D view of their location (a). | 16 |
| Figure 4: Footage of observed damages from the storm Carlos in 2018, used as a calibration on the tilted bathtub approach. Subfigure 'a' represents a beachfront building that had its third store balcony affected, 'b' is the football field that was completely overwashed, 'c' is a building that had severe damages in its structure, and 'd' is the crossroad that had most of the debris from the overwashing concentrated. | 19 |
| Figure 5: Scheme for the tilted bathtub approach, where $h(c)$ is the critical threshold height, R_2 is the runup, α is the coefficient and R_2 tilted is the wave runup height considering the tilting. | 19 |
| Figure 6: Runup values with the validation dataset for Profile 1. | 20 |
| Figure 7: Runup values with the validation dataset for Profile 2. | 21 |
| Figure 8: Runup values with the validation dataset for Profile 3. | 21 |
| Figure 9: Runup calculated with Holman's formula for the time series from 1985 to 2005. The blue, yellow, and green lines represent the values for runup at profiles 1,2, and 3 respectively and the red dotted, dashed and continuous lines are the critical thresholds for profiles 1, 2, and 3, respectively. | 22 |
| Figure 10: Runup calculated with Ruggiero's formula for the time series from 1985 to 2005. The blue, yellow, and green lines represent the values for runup at profiles 1,2, and 3 respectively and the red dotted, dashed and continuous lines are the critical thresholds for profiles 1, 2, and 3, respectively. | 23 |
| Figure 11: Runup calculated with Stockdon's formula for the time series from 1985 to 2005. The blue, yellow, and green lines represent the values for runup at profiles 1,2, and 3 respectively and the red dotted, dashed and continuous lines are the critical thresholds for profiles 1, 2, and 3, respectively. | 23 |

| | |
|--|----|
| Figure 12: Runup calculated with Nielsen's formula for the time series from 1985 to 2005. The blue, yellow, and green lines represent the values for runup at profiles 1,2, and 3 respectively and the red dotted, dashed and continuous lines are the critical thresholds for profiles 1, 2, and 3, respectively | 24 |
| Figure 13: Runup calculated with Voudokas's formula for the time series from 1985 to 2005. The blue, yellow, and green lines represent the values for runup at profiles 1,2, and 3 respectively and the red dotted, dashed and continuous lines are the critical thresholds for profiles 1, 2, and 3, respectively | 24 |
| Figure 14: Runup calculated with Poate's formula, with minimum D_{50} , for the time series from 1985 to 2005. The blue, yellow, and green lines represent the values for runup at profiles 1,2, and 3 respectively and the red dotted, dashed and continuous lines are the critical thresholds for profiles 1, 2, and 3, respectively | 25 |
| Figure 15: Runup calculated with Poate's formula, without D_{50} , for the time series from 1985 to 2005. The blue, yellow, and green lines represent the values for runup at profiles 1,2, and 3 respectively and the red dotted, dashed and continuous lines are the critical thresholds for profiles 1, 2, and 3, respectively | 25 |
| Figure 16: Runup calculated with Poate's formula, with maximum D_{50} , for the time series from 1985 to 2005. The blue, yellow, and green lines represent the values for runup at profiles 1,2, and 3 respectively and the red dotted, dashed and continuous lines are the critical thresholds for profiles 1, 2, and 3, respectively | 26 |
| Figure 17: Runup calculated with Didier's formula for the time series from 1985 to 2005. The blue, yellow, and green lines represent the values for runup at profiles 1,2, and 3 respectively and the red dotted, dashed and continuous lines are the critical thresholds for profiles 1, 2, and 3, respectively | 26 |
| Figure 18: Runup calculated with Power's formula for the time series from 1985 to 2005. The blue, yellow, and green lines represent the values for runup at profiles 1,2, and 3 respectively and the red dotted, dashed and continuous lines are the critical thresholds for profiles 1, 2, and 3, respectively | 27 |
| Figure 19: Runup calculated with Dodet's formula for the time series from 1985 to 2005. The blue, yellow, and green lines represent the values for runup at profiles 1,2, and 3 respectively and the red dotted, dashed and continuous lines are the critical thresholds for profiles 1, 2, and 3, respectively | 27 |
| Figure 20: Return period analysis for Power's formula. | 29 |

Figure 21: Power's formula for runup at storm Carlos (left) considering the topography and bathtub approach (orange) and tilted (red); and the return period of 100 years (right).31

Figure 22: 3D view of the overwash extension using the tilted bathtub approach considering a wave runup of 5 years of the return period.33

List of Tables

| | |
|--|----|
| Table 1: Validation data set oceanic parameters used as inputs for the runup calculation. | 17 |
| Table 2: Runup values for the four formulas that reached the critical thresholds over the validation dataset. | 21 |
| Table 3: Occurrence, maximum values, and average values for the four empirical predictors calculated at the time series from 1985 to 2005. | 28 |
| Table 4: Potential wave Runup (m) for an average profile at different return periods, considering current conditions, an intermediate rise, and a very high rise. | 30 |
| Table 5: Occurrence of flooding events based on the hourly temporal resolution for the three profiles, considering different scenarios of sea-level rise. | 30 |
| Table 6: R2 and overwash extension estimation both with and without the adjustment from the tilted bathtub approach. | 32 |

Index

| | |
|--|-----------|
| Acknowledgements | 7 |
| Abstract | 8 |
| 1. Introduction | 9 |
| 1.1. <i>Wave Runup</i> | 9 |
| 1.2. <i>Wave Overtopping and Overwashing</i> | 12 |
| 1.3. <i>Climate change and Extreme Events</i> | 13 |
| 1.4. <i>Study Site description and morphological/meteo-oceanographic setting</i> | 13 |
| 2. Methodology | 16 |
| 2.1. <i>Wave runup estimation</i> | 16 |
| 2.2. <i>Flood extension estimation</i> | 17 |
| 2.3. <i>Return periods and Climate Change</i> | 18 |
| 3. Results and Discussion | 20 |
| 3.1. <i>Wave runup</i> | 20 |
| 3.2. <i>Return periods and sea-level rise</i> | 29 |
| 3.3. <i>Flood extension</i> | 31 |
| 4. Conclusions | 34 |
| Bibliography | 35 |
| Appendix | 38 |
| <i>Power's formula for wave runup:</i> | 38 |
| <i>Footage of past flooding events at Garachico:</i> | 39 |

Acknowledgments

This thesis had the support from the Erasmus Mundus Joint Master's Degree (EMJMD) program, within the Master's in Water and Coastal Management (WACOMA), that aims at developing common understanding and deepening scientific knowledge in the vital, challenging, and continuously evolving field of water and coastal ecosystems.

I'd like to express my gratitude to my primary supervisor, Dr. Juan, who guided me throughout this project, always supporting and encouraging me to keep pursuing my objectives. My co-supervisor Dr. Haris, for all the support and attention, always with great kindness and dedication. My co-supervisor Dr. Javi, for receiving me in such a prestigious institution, the IH Cantabria, with open arms and for providing me with the data that this work was based on.

Also, my special thanks to the WACOMA coordinators, Prof. Elena Fabbri, Prof. Irene Laiz, and Prof. Alice Newton, who have hosted me with great enthusiasm at the universities of Bologna, Cadiz, and Algarve during these couple of years.

Abstract:

Coastal Hazards are a topic of great interest for managers, given the possible socio-economic consequences associated with them. Specifically, investigating coastal flooding is particularly critical to assess the risk related to extreme ocean events. Also, climate change impacts will potentially increase the risks associated with it. In this sense, a critical parameter to predict the occurrence of flooding in vulnerable areas is the wave runup. In this study, the estimation of wave runup and overtopping were based on several published empirical formulas, derived from field and laboratory experiments, mainly depending on the oceanographic parameters, and the geomorphology of the beach or geometry of the structure. This study aims to 1) investigate the ability of expressions found in the literature to compute wave runup into a rocky and steep bottom at Garachico Island (Spain), by comparing it with past historical events; and 2) assess the risks of coastal flooding based on return periods (response approach) for extreme events using the tilted bathtub approach for evaluating the flooding extension, considering current and future conditions. Moreover, the effect of sea-level rise on different IPCC (Assessment Report 6) scenarios were evaluated. This study will contribute to the development of a methodology to assess coastal flooding, especially for areas characterized by rocky and steep bottoms, which represents a gap in the literature.

Keywords: Coastal Flooding; Coastal Hazards; Risk Assessment; Wave Runup; Overwash; Wave Overtopping; Rocky shorelines; Canary Islands; Climate Change.

1. Introduction

Coastal risks is a topic of great interest for society, given the natural and socioeconomic consequences associated with it. In this sense, investigating wave overtopping and coastal flooding is particularly critical to assess the risk of such events, since it is a severe hazard that leads to loss of lives, assets destruction, and disruption of economic activities (Ferreira, Kupfer, and Costas, 2021). Climate change is also playing an important role in potentializing the vulnerability of this scenario, with rising sea levels and the increase of extreme events both in terms of frequency and intensity. This places the coastal zone, which accounts for 2 percent of the world's land area yet contains 13 percent of the world's urban population (McGranahan, Balk, and Anderson, 2007), at great risk, bringing this matter to attention of the scientific community and managers.

1.1. Wave Runup

Wave runup, defined as the maximum vertical elevation of shoreline water level oscillations caused by ocean waves, is a crucial parameter to evaluate coastal flooding. This is also important for the design of coastal engineering structures and beach morphology since it promotes sediment transportation from the sub-aerial to the submerged beach profile (Gomes da Silva et al., 2020) and the opposite, during storms.

Previous authors (e.g. Holman, 1986) have demonstrated that runup mainly depends on offshore significant wave height (H_0), wave period (T), and wavelength (L_0), linked to the wave period in a linear dispersion relationship, and local beach slope or steepness (β). The Iribarren number (ξ) is a critical non-dimensional parameter based on those three variables. This relationship between these three independent elements allows the characterization of sloped beaches, regarding their wave transformation processes, especially wave breaking, namely: spilling, plunging, collapsing, and surging. Also, it demonstrate how the beach interacts with the waves, in a dissipative, intermediate, or reflective response.

$$L_0 = \frac{gT^2}{2\pi} \quad (1)$$

$$\xi = \tan\beta / \sqrt{H_0/L_0} \quad (2)$$

In early laboratory experiments on wave-driven runup on sloped impermeable structures (Hunt, 1959), it was identified that the wave runup increases with the slope of the structure, and several studies have confirmed this slope dependence in field experiments or through video-based measurements in natural environments (Holman, 1986; Nielsen & Hanslow, 1991; Ruggiero et al., 1991; Vousdoukas et al., 2012). A constant C was established as an empirical coefficient for average ($C = 2.3$) and storm conditions ($C = 3$).

$$(Hunt, 1959) \quad R = CH_0\xi \text{ or } R = C\beta(H_0L_0)^{0.5} \text{ with } 2.3 \leq C \leq 3 \quad (3)$$

$$(Holman, 1986) \quad R_2 = 0.83\tan\beta\sqrt{H_0 + L_0} + 0.2H_0 \quad (4)$$

$$(Nielsen and Hanslow, 1991) \quad R_2 = \begin{cases} 1.0005\beta(H_0L_0)^{0.5} & \text{for } \beta \geq 0.1; \\ 0.0834\beta(H_0L_0)^{0.5} & \text{for } \beta < 0.1 \end{cases} \quad (5)$$

$$(Ruggiero et al. 2001) \quad R_2 = 0.27\sqrt{\beta H_0 L_0} \quad (6)$$

$$(Vousdoukas et al., 2012) \quad R_2 = 0.53\beta\sqrt{H_0L_0} + 0.58\xi\sqrt{H_0^3/L_0} + 0.45 \quad (7)$$

Normally, runup formulas for irregular waves are presented in terms of Runup statistics, such as the maximum runup of the time series (R_{max}), or the runup exceeded by 2% of the waves (R_2). The second one is widely used in the empirical formulas assessed in this paper. A benchmark study for sandy beaches was carried out by Stockdon et al. (2006), where data collected from 10 experiments in multiple swash conditions ($0.07 \leq \xi \leq 3.25$), proposing the most accepted formula to calculate R_2 in sandy beaches (Gomes da Silva et al., 2020).

$$(Stockdon et al., 2006) \quad R_2 = \begin{cases} 1.1 \left(0.35\beta(H_0L_0)^{0.5} + \frac{H_0 + L_0(0.563\beta^2 + 0.004)^{0.5}}{2} \right) & \text{for } \xi > 0.3 \\ 0.043(H_0L_0)^{0.5} & \text{for } \xi < 0.3 \end{cases} \quad (8)$$

While most of the efforts to assess runup empirically were made in sandy beach conditions or wave overtopping on hard defense structures (The EurOtop team, 2018), very few experiments for rocky and steep conditions are found in literature. Poate, McCall, and Masselink (2016) analyzed measurements on gravel beaches with slopes up to 0.4, with the average grain size (D_{50}) also being incorporated in one of the formulas as a bottom friction coefficient. They found a strong relationship with the

offshore significant wave height, decreasing the importance of the beach slope, therefore, the formula from Stockdon et al. (2006) underestimated the runup in their field conditions, since it had a strong dependency on the beach slope.

$$(Poate et al., 2016) \quad R_2 = \begin{cases} 0.21D_{50}^{-0.15}\beta^{0.5}H_0T_{(m-1,0)}H_0 \\ 0.49\beta^{0.5}T_zH_0 \end{cases} \quad (9)$$

According to Dodet et al. (2018), for natural steep rocky cliffs, these dynamics are expected to become even more complex with the higher reflection due to increased steepness, the stronger dissipation due to increased bottom drag, enhanced turbulence during the breaking processes affected by impacts, splash-ups, air entrapment, and the volume loss of the swash discharge due to infiltration within the fractured bedrock. They have investigated the wave runup over steep and irregular rocky profiles in Brittany, France, adapting Hunt's formula by removing the beach slope and implementing an empirical coefficient as described below:

$$(Dodet et al., 2018) \quad R_2 = 0.096(H_0L_0)^{0.5} \quad (10)$$

Didier et al. (2016) also presented a formula to calculate R_{max} for a rocky profile, but in an environment of a rocky shore platform, which induces higher dissipation of the wave energy, followed by a sandy beach profile.

$$(Didier et al., 2016) \quad R_{max} = 1.91H_0\xi_0 + 0.22 \quad (11)$$

Finally, (Power et al. 2019), within the scope of machine learning algorithms, established a genetic-programming-based methodology relying on a compilation of datasets from several prior authors, considering wave steepness, the foreshore slope, and a roughness coefficient ($r = 2.5 D_{50}$). The final formula is too long and was added to an appendix.

$$(Power et al., 2019) \quad x_1 = \frac{H_0}{L_0} \quad x_2 = \beta \quad x_3 = \frac{r}{H_0} \quad (12)$$

Predicting the wave runup is essential to coastal management since it is critical to understand the magnitude of the runup to accurately predict the occurrence of flooding in vulnerable areas. Also, accurate estimates of the runup will allow the effective design of infrastructure for coastal protection (Astorga-Moar and Baldock, 2022).

1.2. Wave Overtopping and Flood Extension

When the wave runup exceeds a critical threshold, considered as the maximum elevation of the protection structure (natural or artificial) in an urbanized context, it induces wave overtopping, characterized by the lens of water from the wave runup that washes over an area that is dry at normal conditions (Sallenger, 2000).

The overwash potential (OP) takes into consideration the wave runup, but also topographic information about the area. It can be estimated through a simple method such as the bathtub approach, which considers the maximum flood elevation exactly as the maximum height of wave runup as a static inundation. Therefore, by forcing the water level on the topography through GIS, it is possible to estimate the flooded area. This approach has some limitations, especially on flat terrains, when a substantial overestimation of the flood extension is made. However, it has its advantages such as low computational costs and simplicity of implementation (Gomes da Silva et al., 2020).

Another solution to evaluate the coastal flooding extension is through dedicated hydrodynamic models (e.g. LISFLOOD-FP), which account for the overtopping discharges and their distribution on the topography, leading to a more accurate result, yet, it also brings more complexity and a high computational cost. The flood intensity index (Dottori, Martina, and Figueiredo 2018) is based on a GIS-based index, which can be considered as a trade-off between morphodynamic indexes and physically based two-dimensional hydraulic models. Also, it is a potential methodology for estimating the flood extension taking into account the effects from the wave runup.

The flood extension can be also computed by a formulation based on flow velocity and observations (Donnelly 2008; Plomaritis, Ferreira, and Costas 2018), and numerical modeling (e.g. Plomaritis, Costas, and Ferreira, 2018). However, even the most realistic numerical or physical models simulations also have their limitations and simplifications. Therefore, a promising way of better understanding the flood extension and having a reasonable estimation for it is by consulting historical footage of past flooding events and incorporating that into an approach based on these observations, as in the tilted bathtub approach (O. Ferreira et al. 2018).

1.3. Climate change and Extreme Events

Many coastal communities around the world are witnessing extreme meteo-oceanographical events, which have raised public awareness of the fact that the climate is constantly changing and having stronger consequences on people's lives, especially comparing it to past decades (Vousdoukas et al. 2016). In terms of coastal hazards, extreme events and climate change both have a major role in this regard, since the occupation of coastal zones was held in a high-pressure context to occupy the closest areas to the ocean, usually not taking into consideration important factors such as erosion and storms.

Traditionally, the management of coastal flooding events has focused on providing protection against it through technical measures aimed at reducing the impacts of a flood episode, by implementing coastal defense structures, for instance. However, a more integrated system for flood risk management, whereby flood risk is defined as the probability of flooding associated with the potential consequences, whether the level of damages, economic losses, or flood extension, for instance, is progressively taken into account (Ward, De Moel, and Aerts, 2011).

In this sense, in an attempt to adapt to this, coastal managers and engineers have implanted an approach based on return periods of storm events for assessing coastal risks and projecting hard defenses. However, it does not completely accounts for some other important factors such as seasonality effects and climate change (Kupfer, Ferreira, and Costas, 2020).

The aim of this study is twofold: the first objective is to investigate the ability of expressions found in literature to compute wave runup into a rocky and steep bottom at Garachico island (Spain) by comparing it with past historical events; and the second is to assess the risks of coastal flooding based on return periods for extreme events using the tilted bathtub approach for current and future conditions according to different IPCC scenarios.

1.4. Study Site description and morphological/meteo-oceanographic setting

Garachico is located Northwest of Tenerife Island (Canary Islands), at 28° 22' 19.70", 16° 45' 54.97" W, as a Spanish out boundary territory in the North Atlantic Ocean (Figure 1). The Canary Islands has been presenting a significant compromise of its

vulnerability to coastal flooding events, given the fast occupation of its littoral as a consequence of the intense interest from the real estate and tourism sectors (Yanes, Marzol, and Romero 2006). Garachico is a remarkable case for wave overtopping assessment, as it has suffered from several coastal flooding events throughout the years.

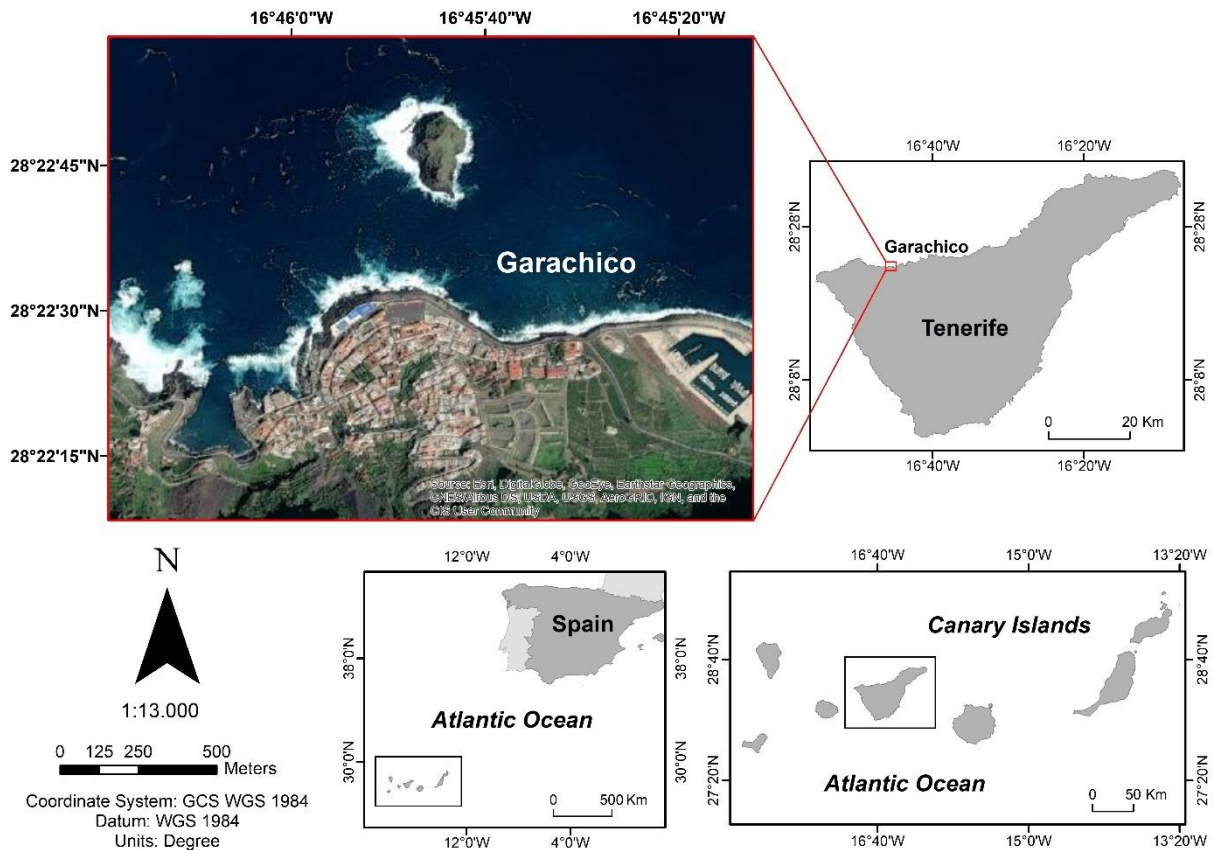


Figure 1: Location map of Garachico, Canary Islands, with a satellite view of the study site.

Its geomorphology is distinctive and originated due to the intense volcanism of the region. It consists of lava rifts deposits from recent times (approximately 20,000 years), more remarkably the eruption from 1706, and its formation is named Dorsal de Abeque (Romero Ruiz and Beltrán Yanes 2015). This geologic background provides Garachico with a rather complex bathymetry, with a very steep slope, and irregular, and rocky bottom, which affects the wave transformation processes.

The Oceanographic conditions are affected by the Canary Island Current, and by the upwelling of the Northwestern African coast, with an average surface temperature of 19°C and salinity of 36.6‰ (Villanueva Guimerans and Ruiz Cañavate 1994). This coast has the influence of the dry Saharan Eastern winds and the North Atlantic trade winds, often from the directions of NNE and NE, with an average speed from 18 to

22km/h, which also influence the wave climate generating sea swells (wave period below 10 seconds), that are more likely to occur in the late autumn until early spring. However, from October to March, there is a predominance of groundswells (wave period up to 20 seconds) with predominant directions from N to (Yanes, Marzol, and Romero 2006).

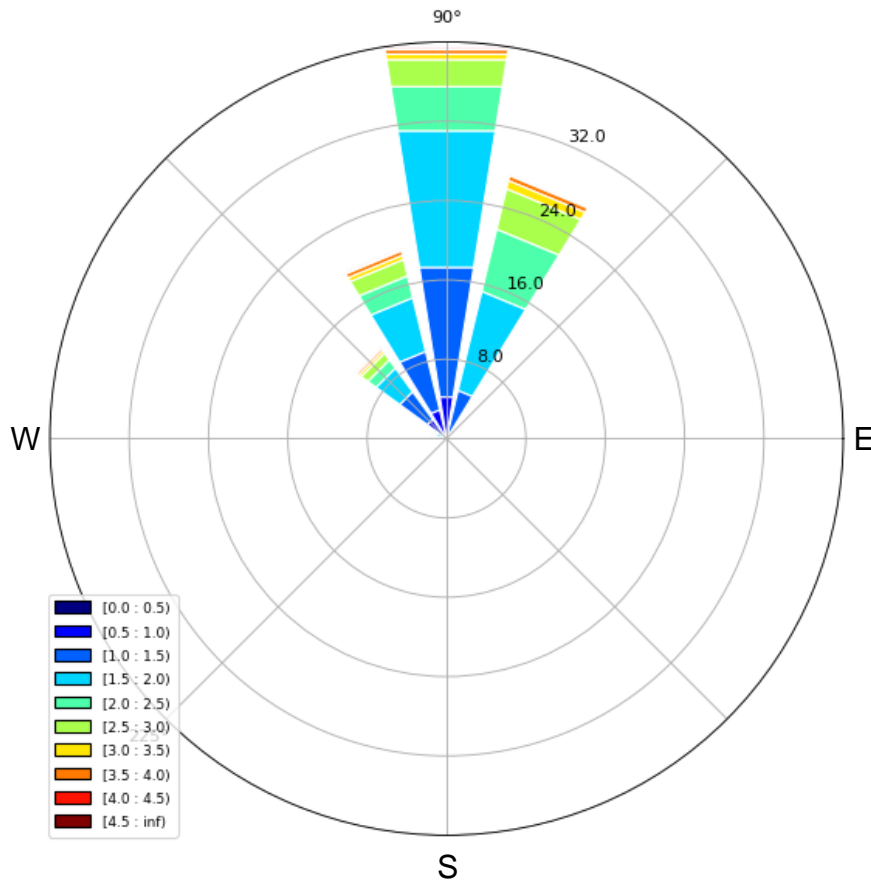


Figure 2: Wind rose representation for the wave climate from 1985 to 2005, showing the main incident wave directions as well as the significant wave height associated with it.

Extreme sea-states have been reported to affect Garachico throughout its history and nowadays, causing high economical loss, as well as offering risk to people, vehicles, roads, and real estate. The Canary Islands, and consequently Garachico, were the areas most affected by the remarkable storm Carlos, on the 18th of November 2018, with significant wave heights up to 6m, leading to the evacuation of 65 residences and several damages (El Confidencial, 2018). The balcony from the third store of a beach-front building at Garachico was reached and damaged by the wave runup, as well as the local football field that was entirely flooded and destroyed, and had to be relocated afterward (Antena 3 Noticias, 2018).

2. Methodology

2.1. Wave runup estimation

A time series for wave climate and sea level from 1985 to 2005, with a high temporal resolution (hourly) at 28° 23' 4.2" N, 16° 46' 10.2" (20m depth) was evaluated. The oceanic conditions were extracted from the database IHDATA from IH-Cantabria, and a high resolution (around 30cm) topo-bathymetric survey was acquired from GRAFCAN. The tides at Garachico have a semidiurnal character ranging from -1.18m to 1.23m in our sample from 1985 to 2005.

Three representative beach profiles were selected to evaluate wave runup through the implementation of empirical predictors, with $\beta_1 = 0.194$; $\beta_2 = 0.161$; and $\beta_3 = 0.159$, which in this thesis is considered as the slope of the swash zone and ± 2 standard deviations of the vertical oscillation of the sea level. The critical thresholds of 9.20m, 8.49m, and 8.02m, respectively, were considered by assessing the local spots where the occupied area is found, either a swimming pool area for profile 2 or a small wall that separates the beach from the main avenue at Garachico (Figure 3).

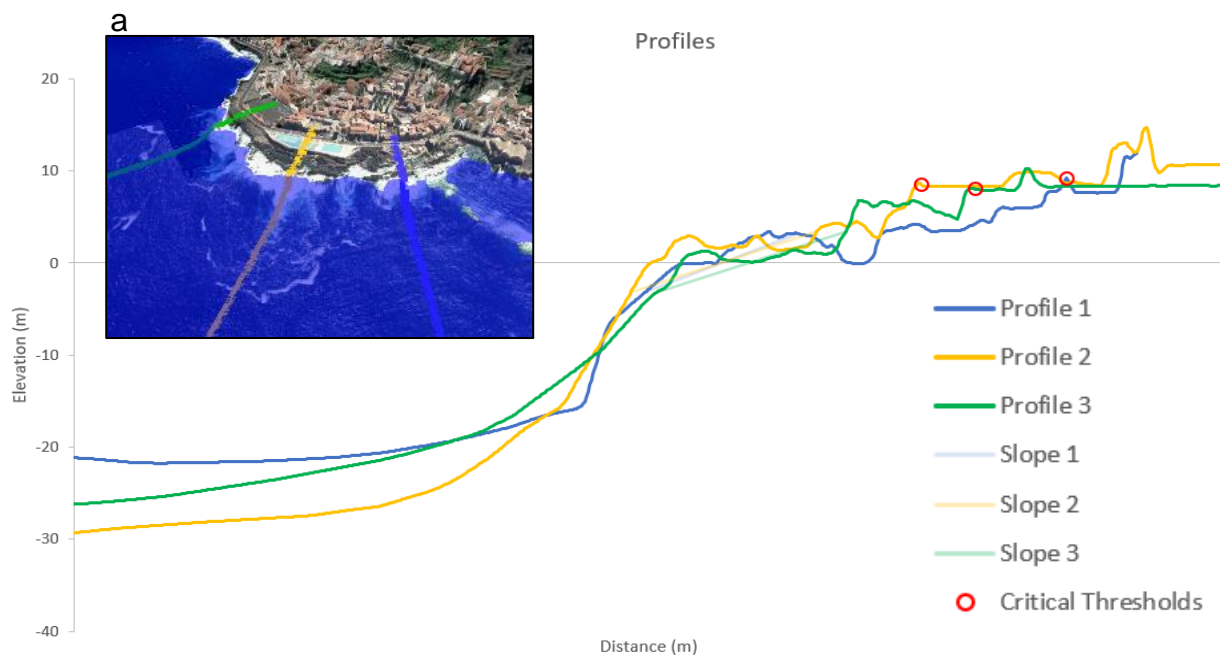


Figure 3: Cross-section representation of the three profiles as well as a 3D view of their location (a).

A cross-validation dataset with storms that demonstrably have presented overwash was also used. This dataset provided by IH Cantabria presents the significant wave height, wave peak period, wave direction, and sea level at five different episodes of

coastal flooding, the first one in November 2018, the storm Carlos mentioned before, and four others in February in the following year.

Table 1: Validation dataset oceanic parameters used as inputs for the runup calculation.

| Date | Hs (m) | Tp (s) | Direction | Tide (m) |
|------------|--------|--------|-----------|----------|
| 18/11/2018 | 5.61 | 19.51 | 328.8 | 0.39 |
| 02/02/2019 | 4.81 | 17.74 | 340.3 | 0.57 |
| 07/02/2019 | 3.87 | 17.74 | 347 | 0.55 |
| 18/02/2019 | 4.68 | 17.74 | 331 | 0.7 |
| 19/02/2019 | 4.61 | 16.13 | 329.3 | 1.01 |

However, not only the assessment of cases that have caused flooding is necessary but also the cases that did not have caused as well, to investigate if the formulas are behaving properly or if there is an overestimation of wave runup in terms of occurrence. Therefore, the wave climate time series from 1985 to 2005 was used to assess the behavior of the empirical predictors throughout Garachico's recent years.

Most of the empirical predictors consider only β , H_0 , and L_0 in its parametrization, however, some consider a roughness or friction parameter like D_{50} , or r ($r = 2.5D_{50}$). Both of these friction parameters rely on the medium grain size, which cannot be determined through field analysis on our site due to the rocky bottom. Therefore, for Poate's formulas, both the maximum (25mm) and the minimum (0.2mm) D_{50} considered in his experiments were carried out in the formulas to evaluate the importance of this parameter in our context. For Power's formula, it was considered the hydraulic roughness length of $3e^{-5}m$, observed by (Howe, 2016) for an asphalt bed.

2.2. Flood extension estimation

For evaluating the risk and intensity of inundation, a simple approach would be to delineate the flooded area through the bathtub approach, which essentially consists of assuming that all the coastal areas connected to the sea with an elevation below the total water level will be inundated (Jiménez et al. 2015). However, this approach leads to an overestimation, since it considers the worst-case scenario, with the volume of overtopping filling the area below the maximum runup quote.

A good strategy to better represent the flooding is adapting the bathtub approach with historical footage of floodings, where the maximum overwash extension is known and it can be related to the matching runup values. In this case, the storm Carlos in 2018, the first case from the validation dataset, completely overwashed the football field at Garachico (Figure 4b), which was used to calibrate the horizontal maximum distance of the flood extension. Also, reports have mentioned that damages were caused at the third store from the beach-front building (Figure 4a), this point being used to evaluate the reached vertical height of the events. These two records were used to calibrate the flooded area and obtain a correction coefficient to reduce the overwash extension, as in the tilted bathtub approach (Jiménez et al., 2015), represented in Figure 5.

2.3. Return periods and Climate Change

A peak over threshold analysis was applied to obtain the cases of the meaningful surplus of runup, and then, a Generalised Pareto Distribution (GPD) was fit to all storm representative runup for a mean profile (averaging profiles 1,2 and 3). Finally, a return period for each threshold of runup was determined with the inverse of the calculated probability according to the length of our time series, which in our case is 21 years (Kupfer, Ferreira, and Costas, 2020). Moreover, two IPCC scenarios were added to the original time-series for sea-level and wave climate, simulating the intermediate (SSP2-4.5) and very high (SSP5-8.5) scenarios for sea-level rise for the year 2120, representing a rise of 0.84m (± 0.36) and 1.15m (± 0.49), respectively. This IPCC data was extracted from the Santa Cruz de Tenerife I datapoint from nasa.gov.



Figure 4: Footage of observed damages from the storm Carlos in 2018, used as a calibration on the tilted bathtub approach. Subfigure (a) represents a beachfront building that had its third store balcony affected, (b) is the football field that was completely overwashed, (c) is a building that had severe damages in its structure, and (d) is the crossroad that had most of the debris from the overwashing concentrated.

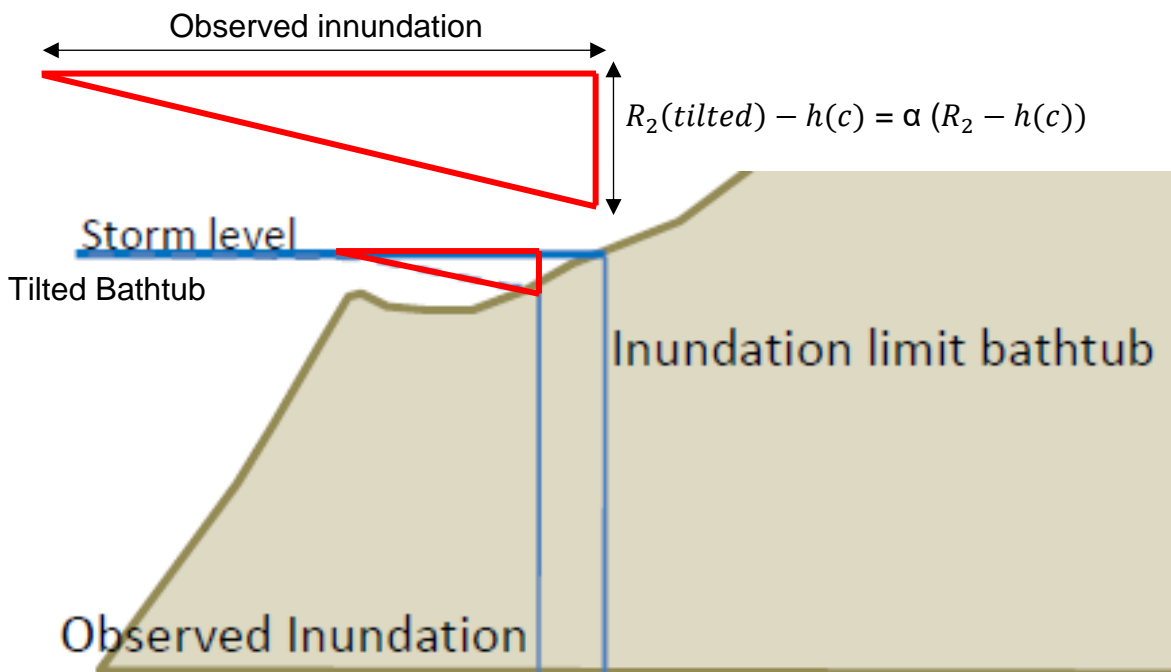


Figure 5: Scheme for the tilted bathtub approach, where $h(c)$ is the critical threshold height, R_2 is the runup, α is the coefficient and R_2 tilted is the wave runup height considering the tilting.

Tilted
Bathtub
Approach

$$\frac{R_2 - h(c)}{R_2(\text{tilted}) - h(c)} = \frac{\text{Calculated length}}{\text{Observed length}} = \quad (12)$$

3. Results and Discussion

3.1. Wave runup

Hereafter it is addressed to the empirical predictors after the name of the first authors. Therefore, the R_2 is calculated using the range of formulas at three representative profiles for 5 different events of validation. According to the validation dataset, it is observed that only the formulas from Power, Nielsen, Poate, and Didier, have reached the critical thresholds for the events that have caused flooding episodes (Figure 6, Figure 7 and Figure 8).

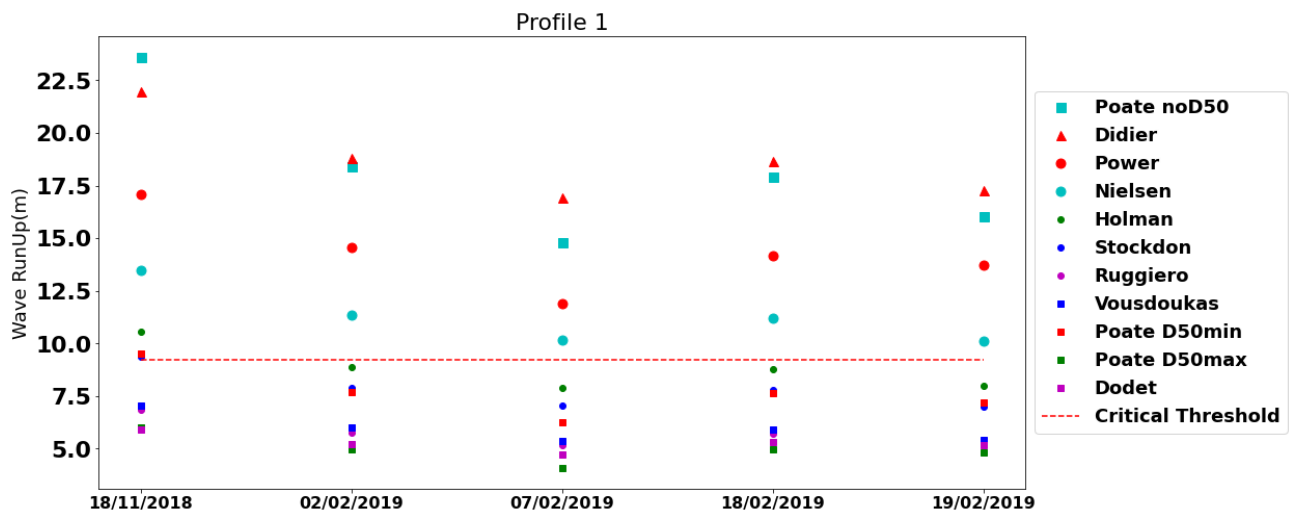


Figure 6: Runup values with the validation dataset for Profile 1.

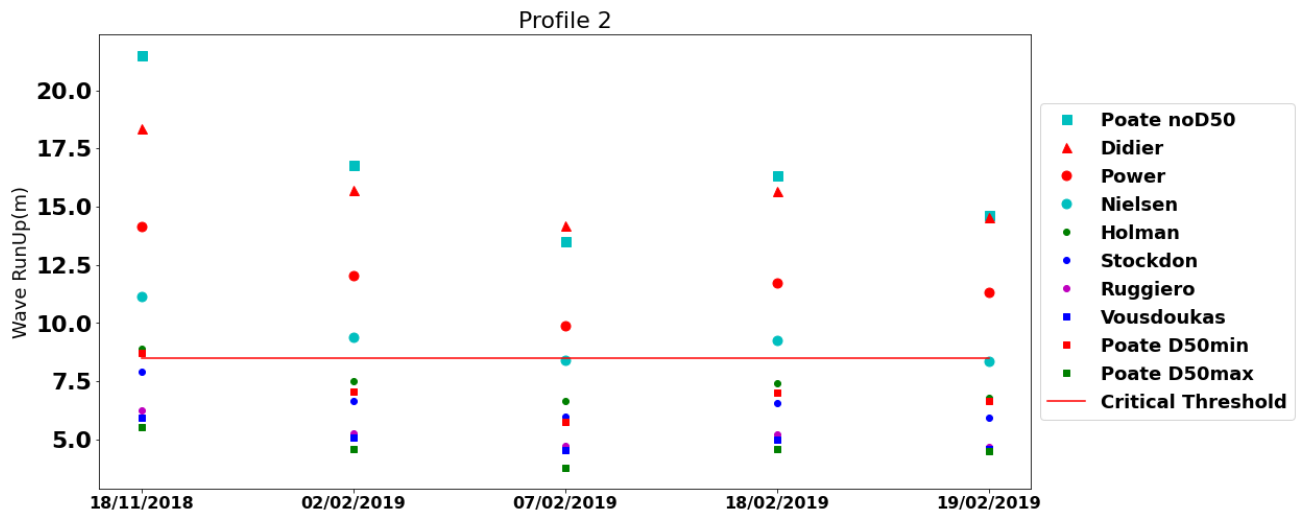


Figure 7: Runup values with the validation dataset for Profile 2.

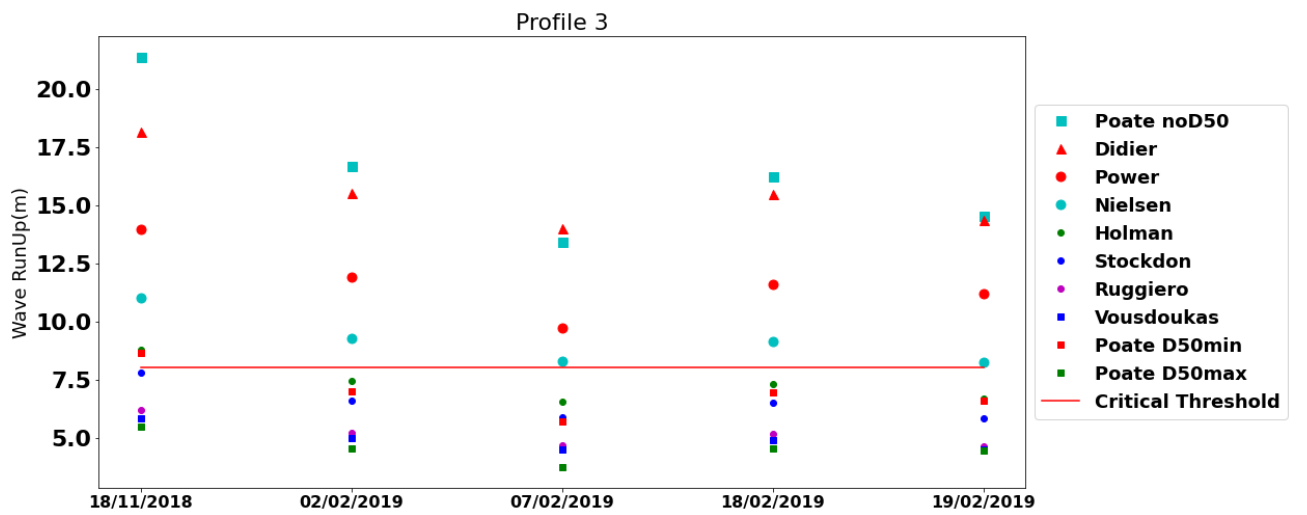


Figure 8: Runup values with the validation dataset for Profile 3.

Table 2: Runup values for the four formulas that reached the critical thresholds over the validation dataset.

| Empirical Predictors | Profile 1 | | | | Profile 2 and 3 | | | |
|----------------------|-----------|-------|--------|-------|-----------------|-------|--------|-------|
| | Nielsen | Power | Didier | Poate | Nielsen | Power | Didier | Poate |
| 18/11/18 | 13.5 | 17.1 | 22.0 | 23.6 | 11.1 | 14.1 | 18.4 | 21.5 |
| 02/02/19 | 11.3 | 14.5 | 18.8 | 18.4 | 9.4 | 12.0 | 15.7 | 16.8 |
| 07/02/19 | 10.2 | 11.9 | 16.9 | 14.8 | 8.4 | 9.8 | 14.2 | 13.5 |
| 18/02/19 | 9.1 | 14.2 | 18.7 | 17.9 | 9.2 | 11.7 | 15.7 | 16.3 |
| 19/02/19 | 11.2 | 13.7 | 17.2 | 16.0 | 8.3 | 11.3 | 14.5 | 14.6 |

Poate's formula that does not consider D_{50} (eq. 9.2) has presented the highest results for runup, reaching values up to 23.6m, followed by Didier, with values up to 22m, Power, with values up to 17.1m and Nielsen, with values up to 13.5m for profile 1. Profiles 2 and 3 has essentially the same slope, therefore, the runup at both was practically the same. However, Profile 2 has a slightly higher critical threshold, which makes the results for the third and fifth episode from the validation dataset almost reach the flooding quote, though staying slightly below this mark.

The wave climate hindcast from 1985 to 2005 was also evaluated for all the empirical predictors, as represented in Figure 9 to Figure 19 for all the formulas, especially the four formulas that have reached the critical thresholds for the validation dataset (Figures 6, 7 and 8), this is important for the evaluation of the behavior of the formulas in terms of occurrence rate, meaning that a formula that has presented a positive case for overtopping in the validation dataset, could potentially present overtopping in excess for the hindcast, leading to an overestimation of flooding events.

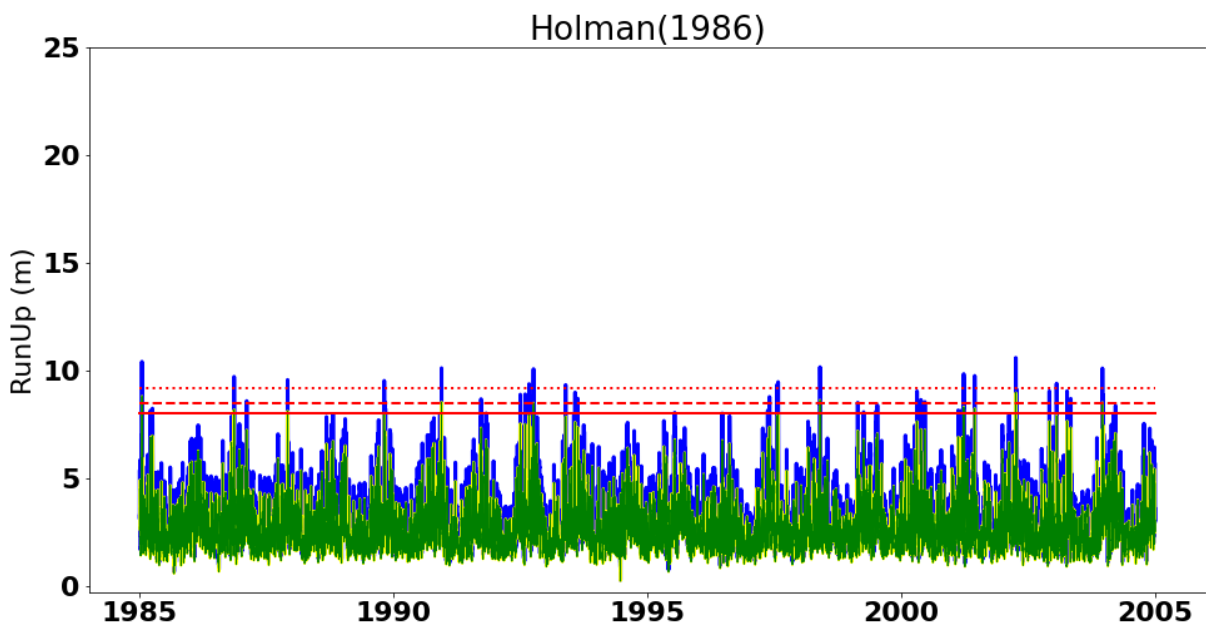


Figure 9: Runup calculated with Holman's formula for the time series from 1985 to 2005. The blue, yellow, and green lines represent the values for runup at profiles 1, 2, and 3 respectively and the red dotted, dashed and continuous lines are the critical thresholds for profiles 1, 2, and 3, respectively.

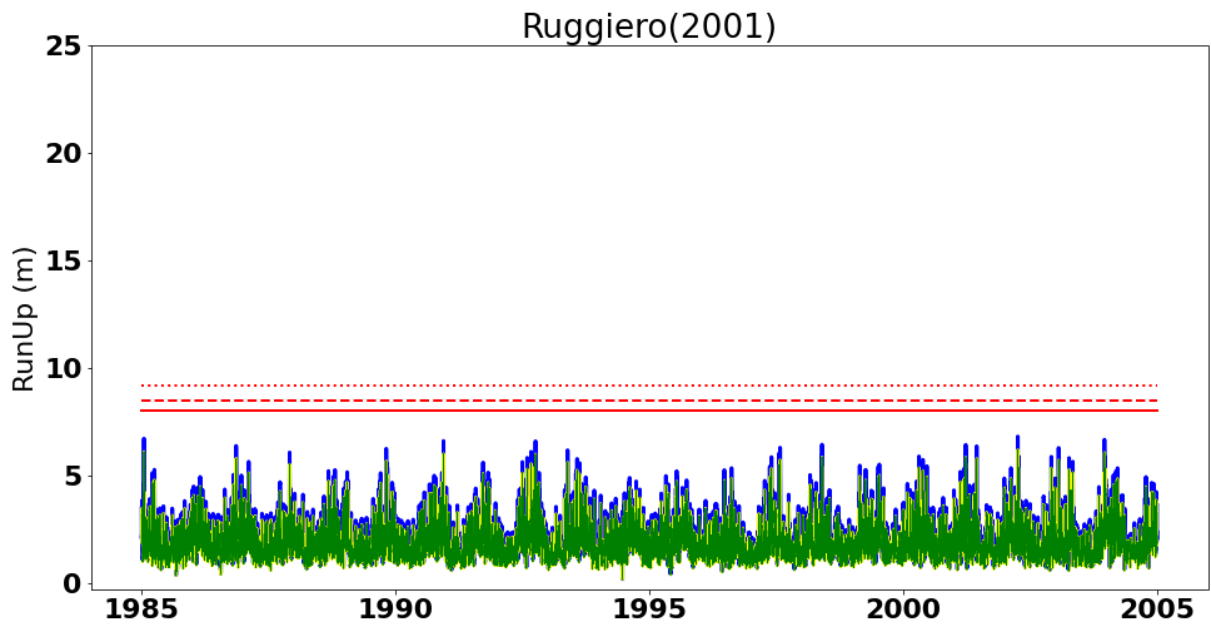


Figure 10: Runup calculated with Ruggiero's formula for the time series from 1985 to 2005. The blue, yellow, and green lines represent the values for runup at profiles 1,2, and 3 respectively and the red dotted, dashed and continuous lines are the critical thresholds for profiles 1, 2, and 3, respectively

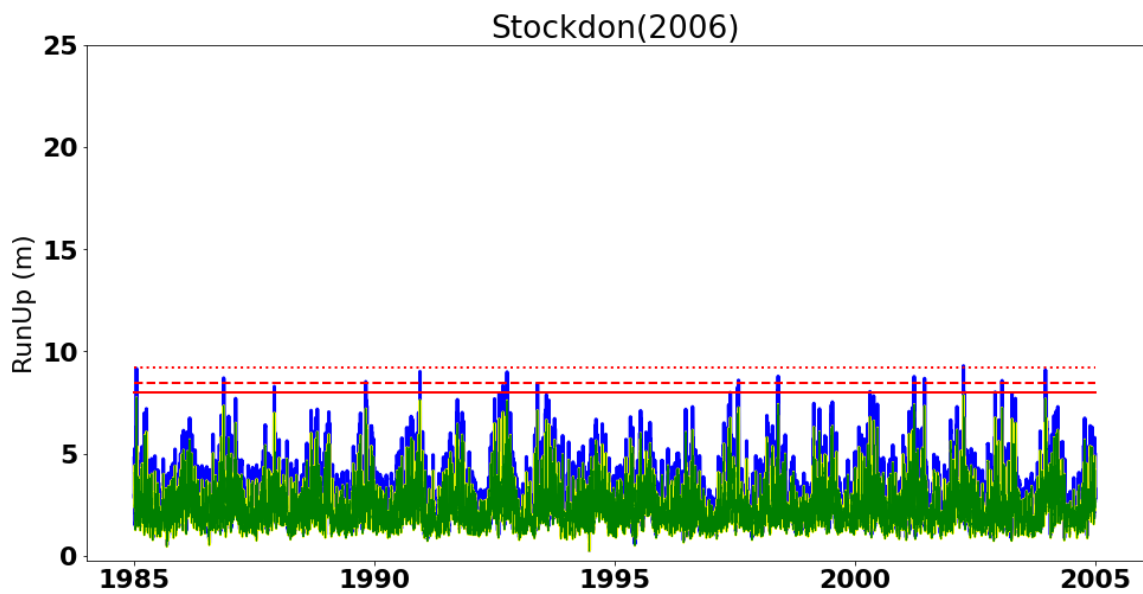


Figure 11: Runup calculated with Stockdon's formula for the time series from 1985 to 2005. The blue, yellow, and green lines represent the values for runup at profiles 1,2, and 3 respectively and the red dotted, dashed and continuous lines are the critical thresholds for profiles 1, 2, and 3, respectively

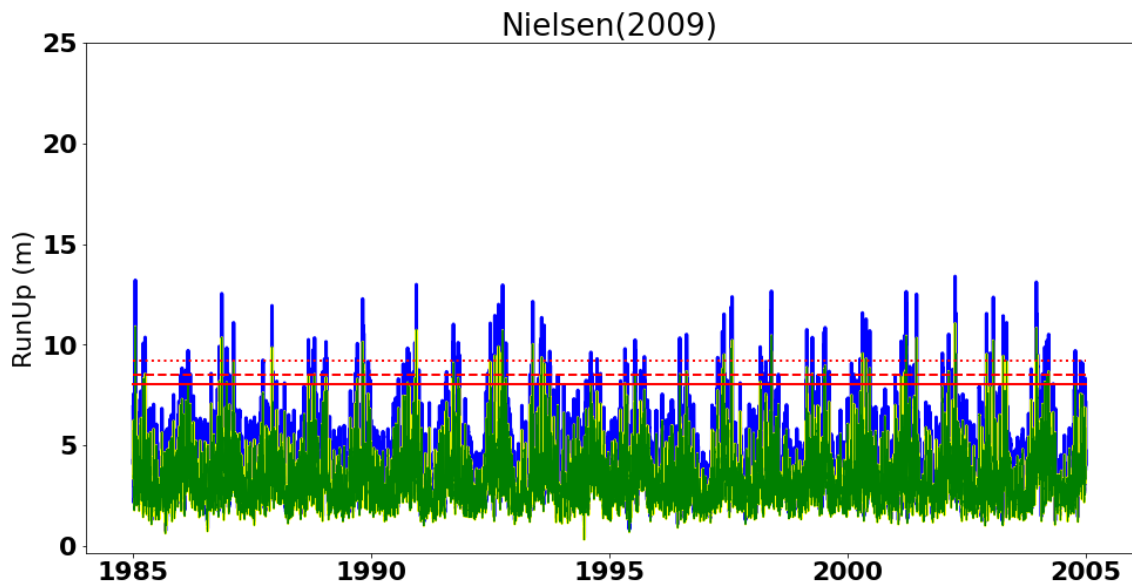


Figure 12: Runup calculated with Nielsen's formula for the time series from 1985 to 2005. The blue, yellow, and green lines represent the values for runup at profiles 1, 2, and 3 respectively and the red dotted, dashed and continuous lines are the critical thresholds for profiles 1, 2, and 3, respectively

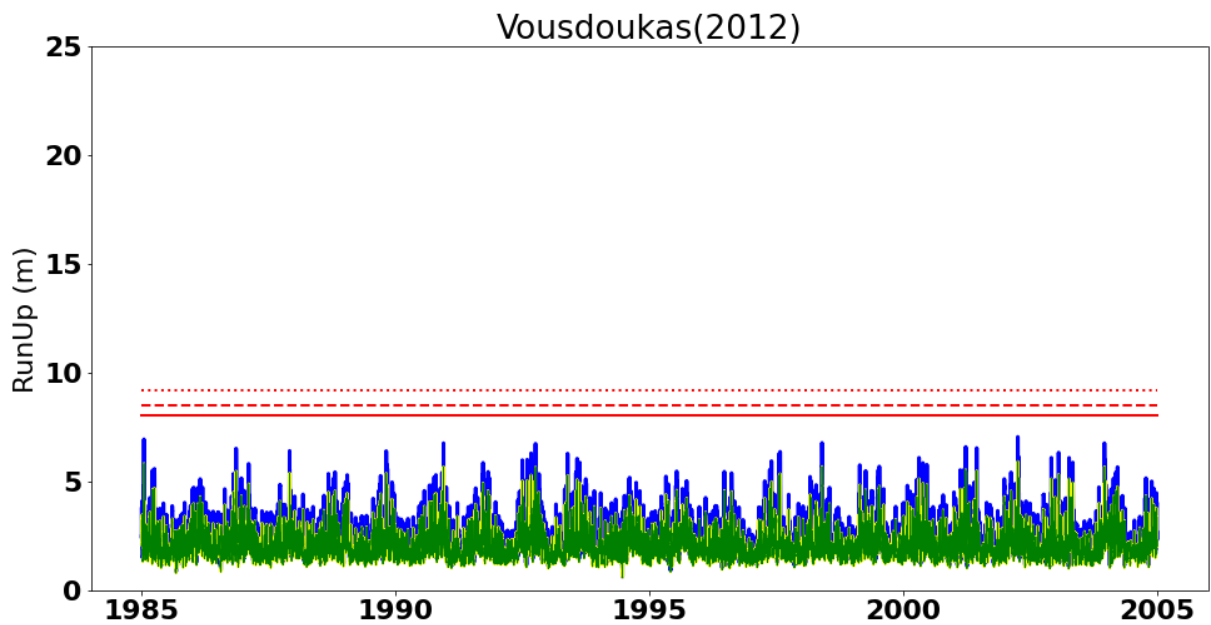


Figure 13: Runup calculated with Vousdokus's formula for the time series from 1985 to 2005. The blue, yellow, and green lines represent the values for runup at profiles 1, 2, and 3 respectively and the red dotted, dashed and continuous lines are the critical thresholds for profiles 1, 2, and 3, respectively

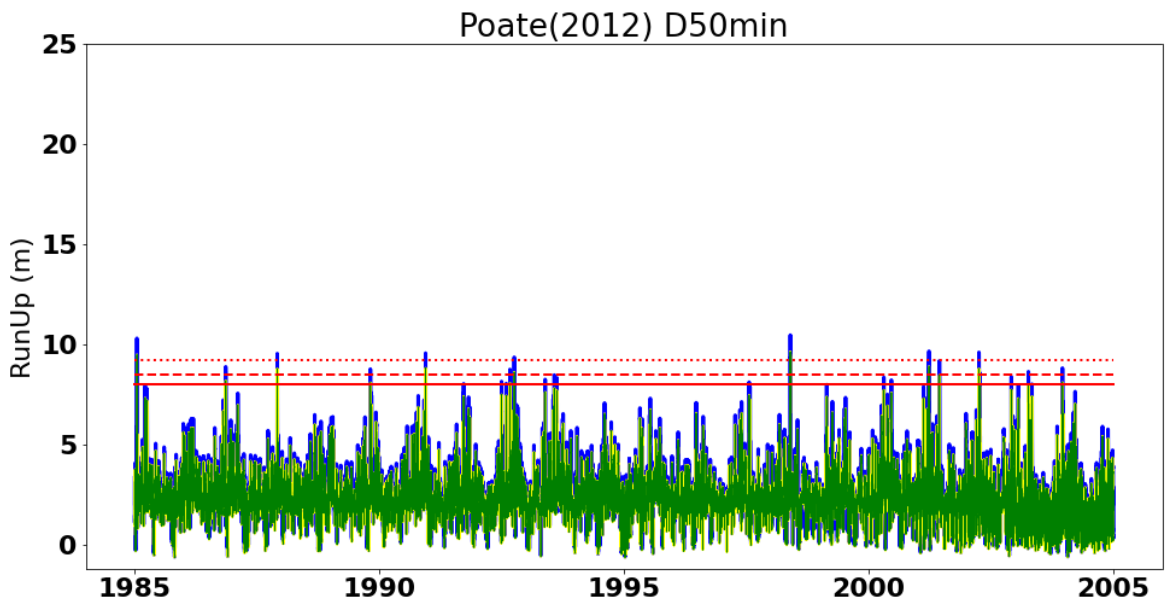


Figure 14: Runup calculated with Poate's formula, with minimum D_{50} , for the time series from 1985 to 2005. The blue, yellow, and green lines represent the values for runup at profiles 1, 2, and 3 respectively and the red dotted, dashed and continuous lines are the critical thresholds for profiles 1, 2, and 3, respectively

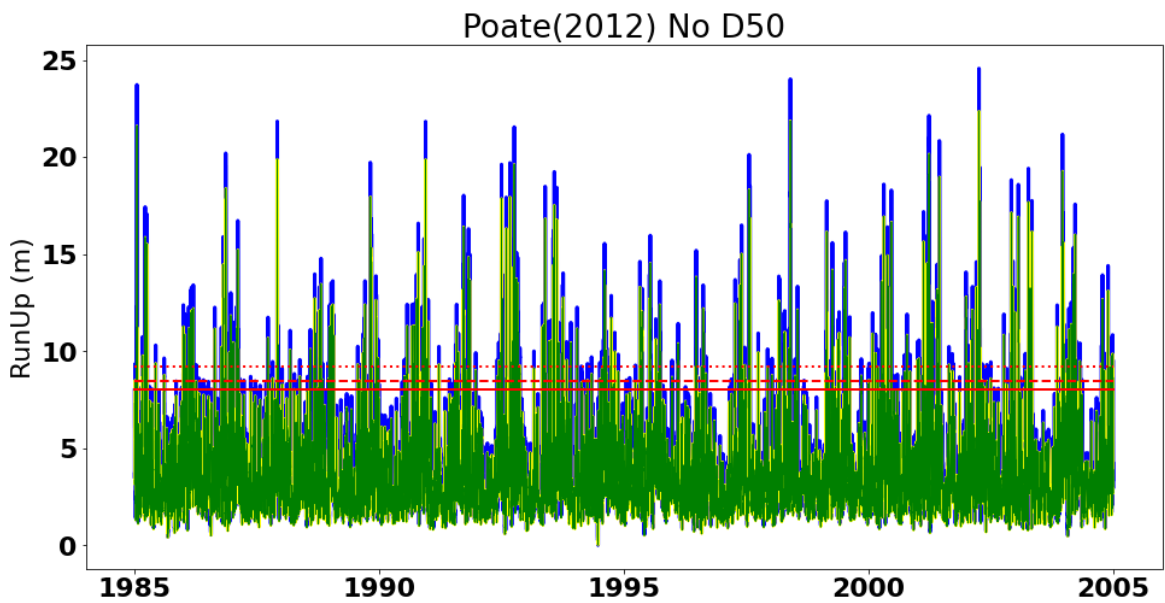


Figure 15: Runup calculated with Poate's formula, without D_{50} , for the time series from 1985 to 2005. The blue, yellow, and green lines represent the values for runup at profiles 1, 2, and 3 respectively and the red dotted, dashed and continuous lines are the critical thresholds for profiles 1, 2, and 3, respectively

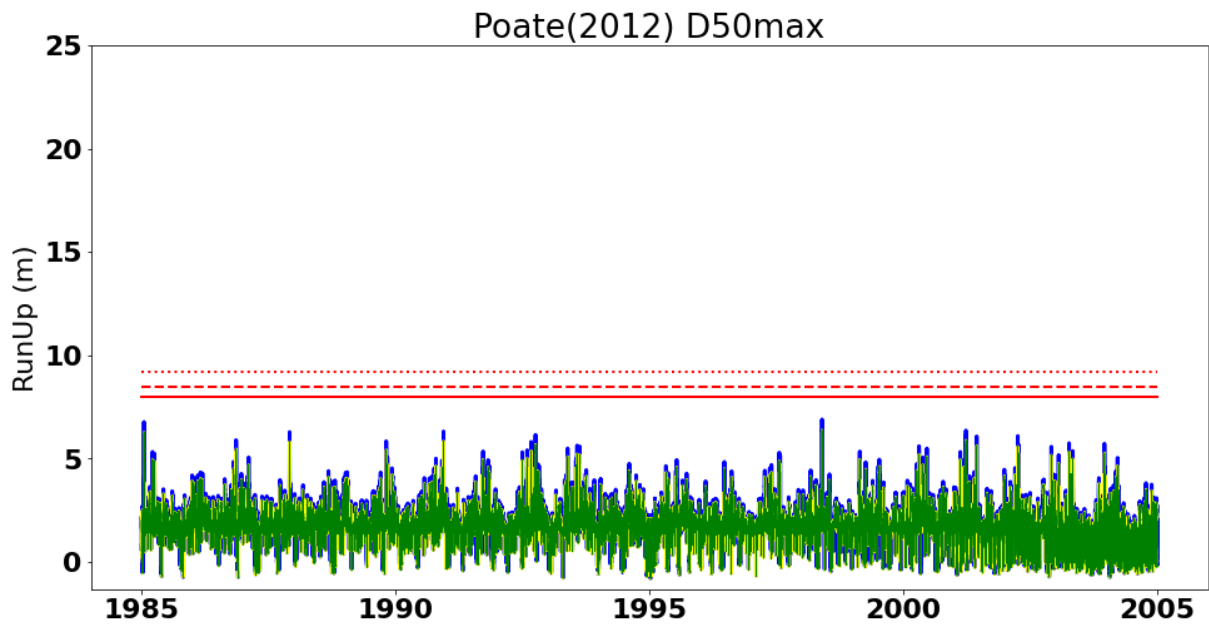


Figure 16: Runup calculated with Poate's formula, with maximum D_{50} , for the time series from 1985 to 2005. The blue, yellow, and green lines represent the values for runup at profiles 1, 2, and 3 respectively and the red dotted, dashed and continuous lines are the critical thresholds for profiles 1, 2, and 3, respectively

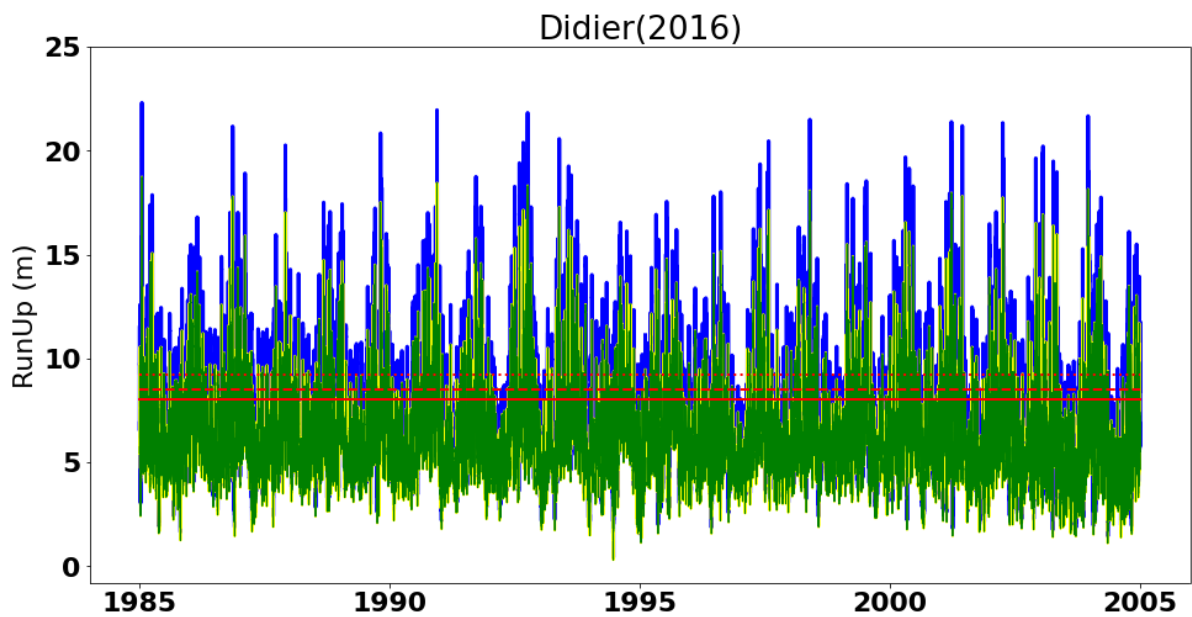


Figure 17: Runup calculated with Didier's formula for the time series from 1985 to 2005. The blue, yellow, and green lines represent the values for runup at profiles 1, 2, and 3 respectively and the red dotted, dashed and continuous lines are the critical thresholds for profiles 1, 2, and 3, respectively

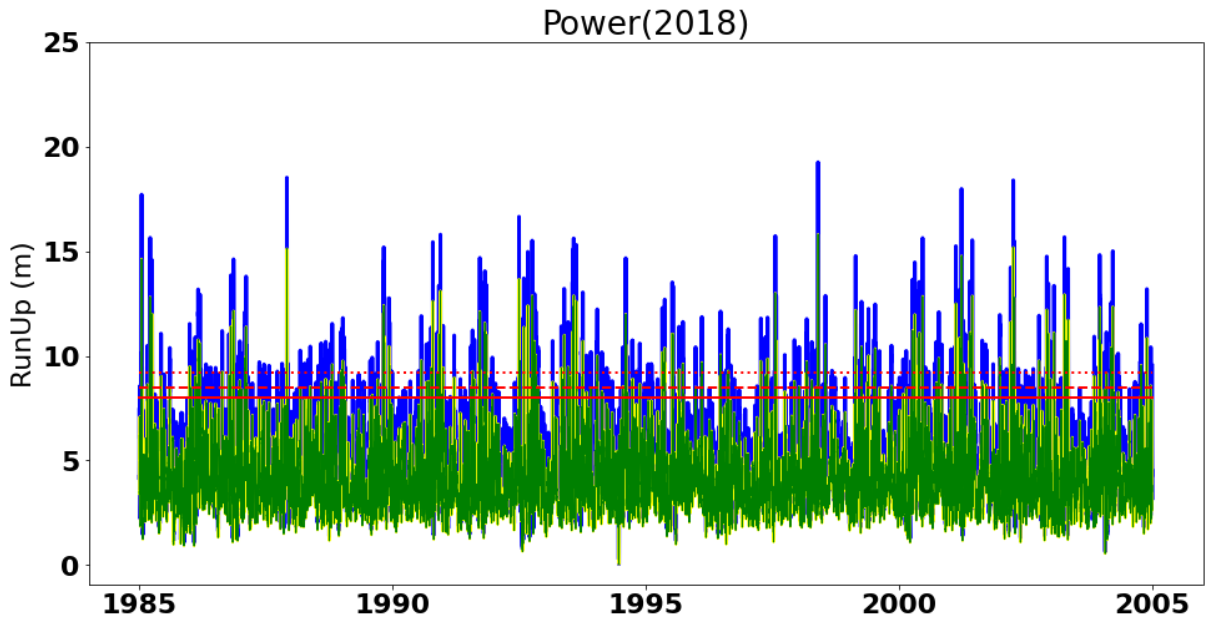


Figure 18: Runup calculated with Power's formula for the time series from 1985 to 2005. The blue, yellow, and green lines represent the values for runup at profiles 1,2, and 3 respectively and the red dotted, dashed and continuous lines are the critical thresholds for profiles 1, 2, and 3, respectively

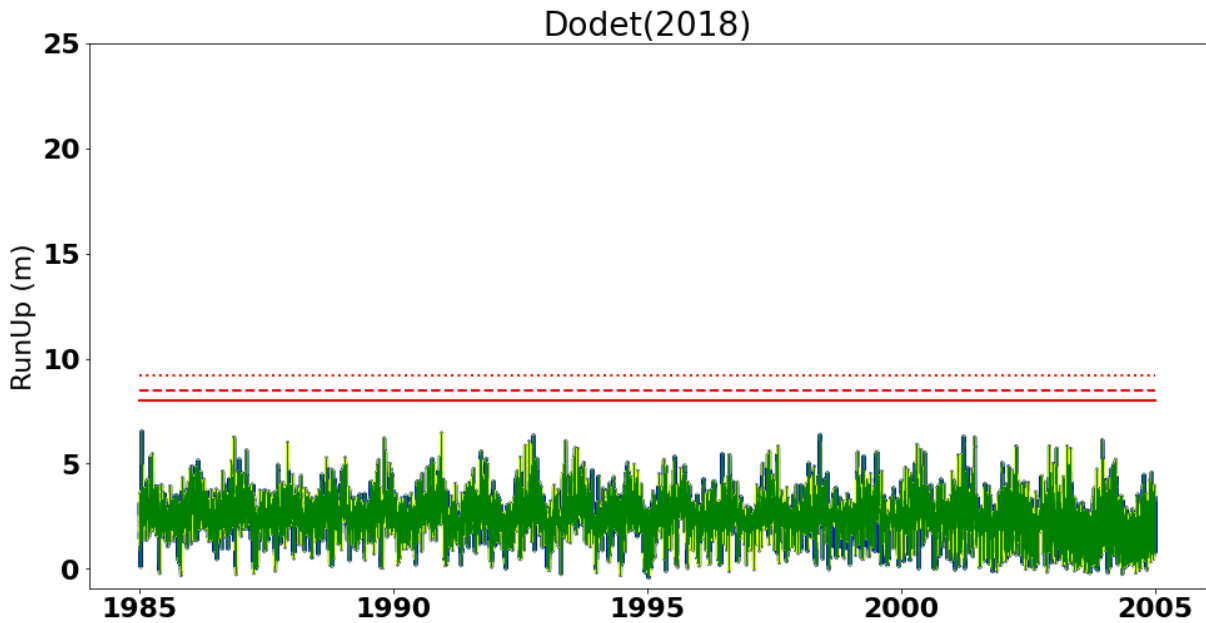


Figure 19: Runup calculated with Dodet's formula for the time series from 1985 to 2005. The blue, yellow, and green lines represent the values for runup at profiles 1,2, and 3 respectively and the red dotted, dashed and continuous lines are the critical thresholds for profiles 1, 2, and 3, respectively

Table 3: Occurrence, maximum values, and average values for the four empirical predictors calculated at the time series from 1985 to 2005.

| Empirical Predictors | Profile 1 | | | Profile 2 | | | Profile 3 | | |
|----------------------|------------|---------|-------------|------------|---------|-------------|------------|---------|-------------|
| | Occurrence | Max (m) | Average (m) | Occurrence | Max (m) | Average (m) | Occurrence | Max (m) | Average (m) |
| Nielsen | 1.02% | 13.40 | 4.12 | 0.42% | 11.07 | 3.41 | 0.70% | 11.07 | 3.41 |
| Poate | 4.30% | 24.56 | 4.17 | 4.10% | 22.37 | 3.80 | 5.05% | 22.37 | 3.80 |
| Didier | 22.74% | 22.30 | 7.61 | 15.90% | 18.74 | 6.50 | 20.61% | 18.74 | 6.50 |
| Power | 3.87% | 19.26 | 5.08 | 2.22% | 15.81 | 4.18 | 2.94% | 15.81 | 4.18 |

Since profile 1 has a steeper beach slope, the runup is more intense at it, supporting the results of prior authors. This profile is also tilted towards the west, meaning that the waves do not hit it normally, but with an angle, which tends to alter the wave transformation reducing its impact. Therefore, a propagation of the wave climate closer to it would be recommendable, followed by a reverse shoaling equation to obtain the equivalent offshore wave parameters (Plomaritis, Ferreira, and Costas 2018). Alternatively, a reduction factor to the significant wave height (Galland 1994; Wolters and Van Gent 2011), or the mean overtopping discharge (The EurOtop team 2018), could also be implemented. As expected, it presented the highest values for occurrence, ranging from 1.02% to 22.74%, maximum and average runup, from 13.40m to 24.56m and from 4.12m to 5.08m, respectively (Table 3).

Profiles 2 and 3 has the same slope, however, they have slightly different critical thresholds for flooding, and, therefore, the occurrence of overtopping events is different between them, although the maximum and average runup are the same. The occurrence ranged from 0.42% up to 15.90% for Profile 2, while Profile 3 varied from 0.70% to 20.61%, and the maximum runup was from 11.07m to 22.37m with the average values from 3.41m to 6.50m for both Profiles.

Nielsen has presented the smaller values in all 3 Profiles for occurrence, maximum runup, and average runup. This may indicate an underestimation, especially compared to the validation dataset, since it does not reach the critical threshold for Profiles 2 and 3 in two out of the 5 validation storms. Poate's formula has presented the highest values for maximum runup, including in the validation dataset, which might indicate an overestimation in his formula.

Didier has presented the second highest values for maximum runup, however, its occurrence and average is critically high, resulting in an unrealistic occurrence of overtopping. Finally, Power has indicated the second-lowest occurrence rate and a coherent maximum runup, when comparing the validation dataset with actual levels of damages under those circumstances, like reaching the third store of the beachfront building (Figure 4a) and overwashing the whole football field. Therefore, it presents the best fit among them.

3.2. Return periods and sea-level rise

Considering Power (2018) as the most accurate empirical runup predictor, it is proceed to the evaluation of the return periods and IPCC scenarios. For practicality, an average wave runup was considered by using the mean runup of the three profiles, and the average critical threshold of 8.57m.

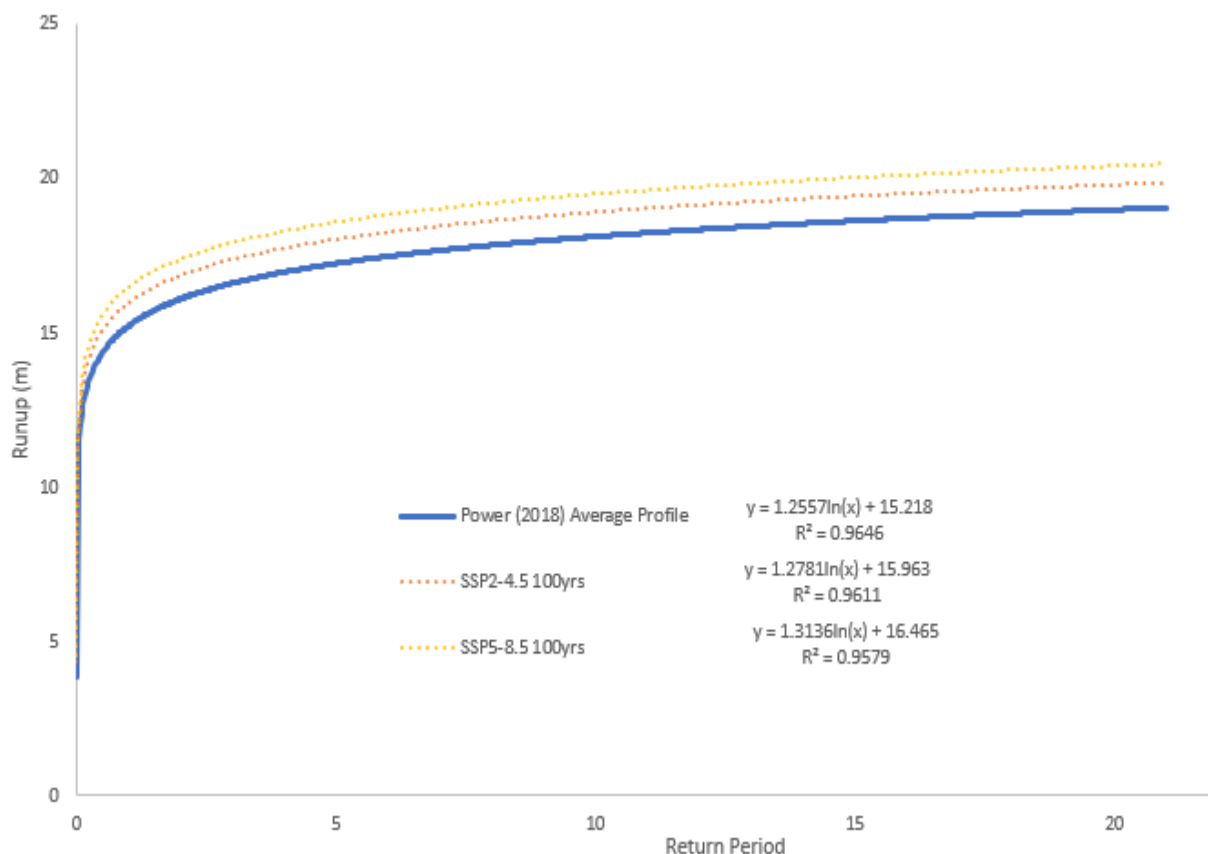


Figure 20: Return period analysis for Power's formula.

Three scenarios were evaluated, the first one considers current conditions, the SSP2-4.5 considers that no significant additional climate policy would be added to the current

scenario. Therefore, it is an estimation based on today's standards for sea-level rise, and the SSP5-8.5 is considered as a high reference scenario with no additional climate policy but with the emission levels increasing. The values for sea-level rise at the year 2120 were added to our sea-level time series from 1985 to 2005 and the return period analysis was held considering them (Table 4).

Table 4: Potential wave Runup (m) for an average profile at different return periods, considering current conditions, an intermediate rise, and a very high rise.

| Return Period (years) | R_2 (m) | R_2 SSP2-4.5 (m) | R_2 SSP5-8.5 (m) |
|--------------------------|-----------|-----------------------|-----------------------|
| 5 | 17.24 | 17.99 | 19.28 |
| 10 | 18.12 | 18.88 | 19.49 |
| 25 | 19.26 | 20.04 | 20.69 |
| 50 | 20.13 | 20.93 | 21.60 |
| 100 | 21.00 | 21.82 | 22.51 |

Table 5: Occurrence of flooding events based on the hourly temporal resolution for the three profiles, considering different scenarios of sea-level rise.

| Profiles | Occurrence | | |
|----------|------------|----------|----------|
| | No SLR | SSP2-4.5 | SSP5-8.5 |
| 1 | 3.87% | 6.43% | 7.20% |
| 2 | 2.22% | 3.71% | 4.21% |
| 3 | 2.94% | 5.15% | 5.86% |

The return period analysis of the extreme values for wave runup using Power's formula has presented values up to 21m high for a 100-year return period. However, the smallest return period of 5 years already has presented alarming values for wave runup (17m), which is very close to the storm Carlos from the validation dataset that has caused great damage. Therefore, the highest probability of occurrence evaluated already has a high level of damage, leading Garachico into a great vulnerability.

According to the IPCC projections, the sea-level rise will play a crucial role in the occurrence of coastal flooding events in Garachico. The difference on maximum wave runup would increase a maximum of 2.04m in the worst-case scenario for a projection for the year 2120 with runup events within 5 years of the return period, leading to damages expected from 25 years of return period runup. Moreover, with the same wave climate but in the year 2120, the occurrence of overtopping events would almost

double for the worst-case scenario of sea-level rise, meaning that the frequency of flooding will be severely increased.

3.3. Flood extension

Based on historical footage of the past flooding event in November 2018 (Figure 4), the storm Carlos, which is our first event from the validation dataset, the levels of overwash extension were compared to the extensions of flooding from the Power's formulation and adjusted by using a reduction coefficient as explained in Figure 5, using the tilted bathtub approach

At this event, the football field, which has a horizontal extension from the critical threshold to its end of approximately 80m, was completely overwashed, while the Power's formula for run-up was presenting an overwash extension of around 190m. Therefore, a coefficient for the tilted bathtub approach of $\alpha = 0.42$ was obtained. The coefficient α is obtained through the adjustment of the horizontal extension based on observation of this past flooding event. However, for the flood map, this coefficient is applied to the vertical height of the runup above the critical threshold, as represented in the left part of Equation 12.

It is clear the significant reduction of the extension of the flooded area in Figure 21, where on the left is represented the storm Carlos, and on the right is an event with a 100-year return period. This is essential for calibrating the extension of the flood, which otherwise would be overestimated if using the regular bathtub approach.

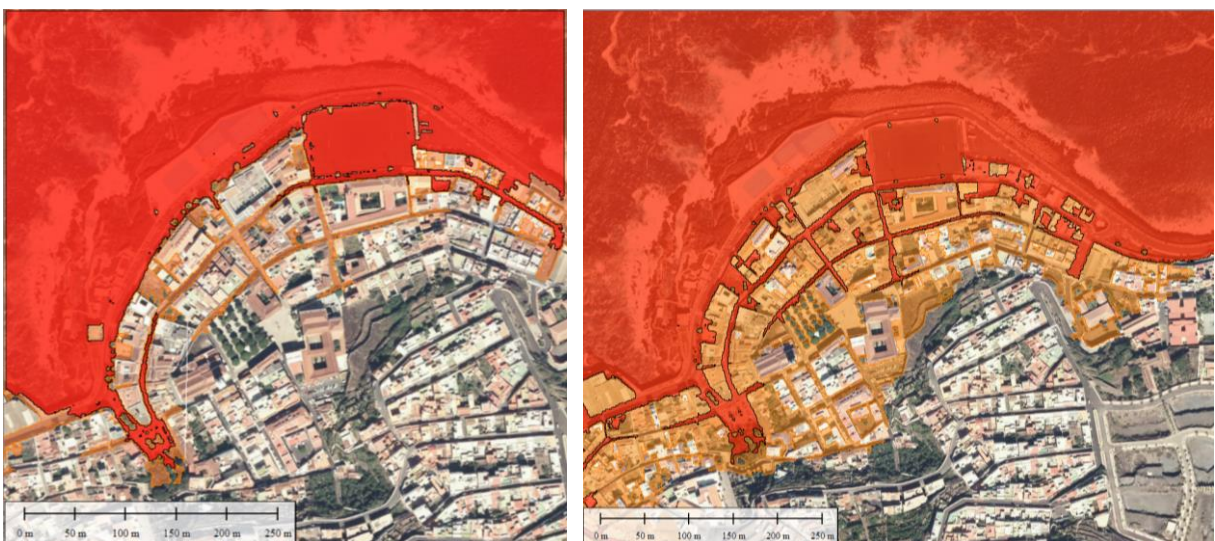


Figure 21: Power's formula for runup at storm Carlos (left) considering the topography and bathtub approach (orange) and tilted (red); and the return period of 100 years (right).

By using this coefficient, the results for the flooding area with Power’s formula at storm Carlos were very close to the reality of the episode, accounting for an accurately similar area as seen in the *in situ* footage (see appendix). In Table 6, the mean R_2 from Power’s formula for the 5 return periods and the adjusted R_2 from the tilted bathtub approach is presented, as well as an overwash extension estimation for the football field section, both without and with the coefficient α .

Table 6: R_2 and overwash extension estimation both with and without the adjustment from the tilted bathtub approach.

| Return Period (years) | R_2 (m) | R_2 Tilted (m) | Overwash extension (m) | Overwash extension tilted (m) |
|-----------------------|-----------|------------------|------------------------|-------------------------------|
| 5 | 17.24 | 12.21 | 245 | 135 |
| 10 | 18.12 | 12.58 | 251 | 137 |
| 25 | 19.26 | 13.06 | 254 | 180 |
| 50 | 20.13 | 13.42 | 255 | 185 |
| 100 | 21.00 | 13.79 | 261 | 190 |

The bathtub approach does not account for processes such as flow velocity or discharge, infiltration or friction, as so it does the tilted bathtub approach, however, adding the empirical coefficient to the vertical length of runup based on prior flooding events adds a stronger connection with the reality. Since Garachico is backed by dense infrastructure behind the critical thresholds, like asphalt roads and houses, mostly impermeable, this approach tends to behave better when compared to sandy or gravel beaches.

A more robust methodology, based on *in situ* measurements through camera monitoring, for instance, and possibly coupling the wave runup results with a 2D hydrodynamic numerical model to analyze the flow of the overtopping discharge direction and volume, incorporating the terrain topography and morphology characteristics, could add even more accuracy. Although often adding technical robustness does not necessarily improve the results, since it might also bring simplification, errors, and inconsistencies. However, unquestionably a better survey of past flood events would add more reliability to these results.

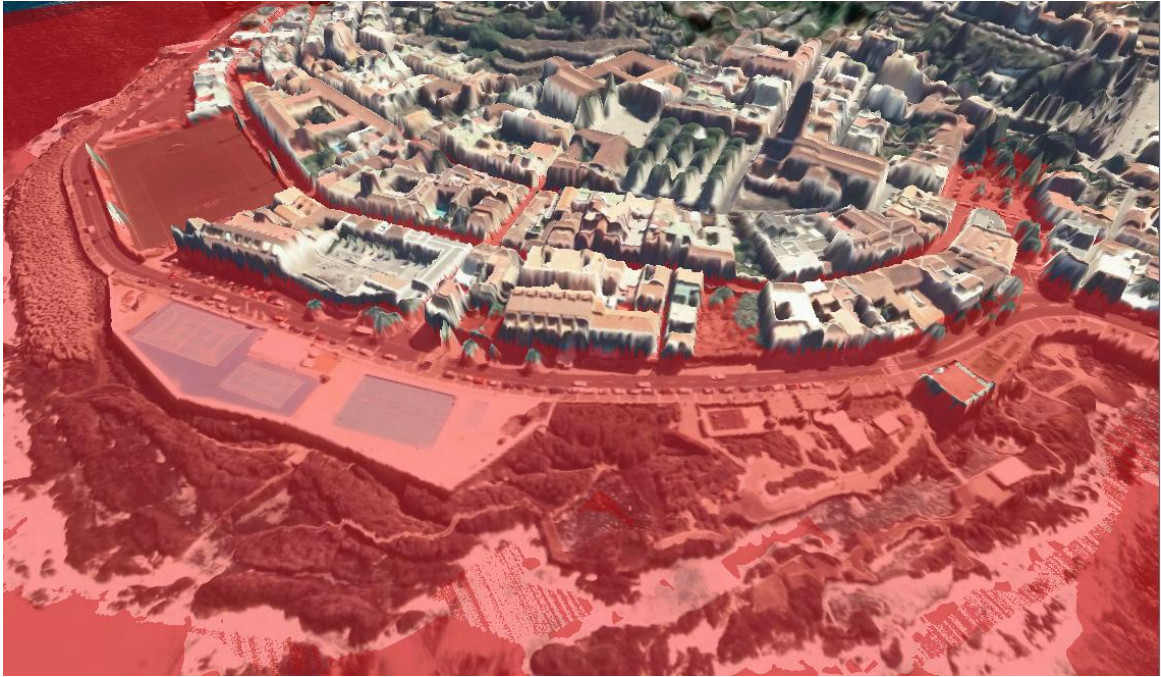


Figure 22: 3D view of the overwash extension using the tilted bathtub approach considering a wave runup of 5 years of the return period.

For a detailed risk analysis, normally is required a coherent characterization of the region in multiple aspects, such as economics, social, and cultural. However, the flood map is an essential tool given it represents the potentially affected areas, although without considering its value. According to our floodmap and overwash extension, all the first line of occupation in the beachfront road (Av. Tomé Cano/Av. Adolfo Suárez) is dramatically at risk, while the second street (Calle Esteban de Ponte) also presented overwash in some extent.

Even considering the reduction coefficient from the tilted bathtub approach, this methodology may still present some overestimations according to the limitations already discussed. Nevertheless, due to its low computational effort, it becomes a promising alternative when compared to dynamic inundation modeling, especially for larger scales and when data access is limited (Michalis I. Vousdoukas et al. 2016). Future works can improve this incipient methodology by implementing larger data-sets of previous flooding events and a dynamic coefficient, for instance.

4. Conclusions

Garachico has very distinctive characteristics, given its rocky, steep, and irregular bottom, representing a gap in the literature of wave runup and coastal flooding risk assessment. This study has presented an evaluation of 11 empirical predictors for wave runup, throughout a time series of 21 years of wave and sea-level data, as well as a validation dataset of past flooding events.

The formula that presents the most accurate results is based on genetic-programming algorithms (Power et al. 2019) and accounts for a wide range of datasets from multiple authors and cases, giving a probabilistic bias to a rather deterministic way to estimate runup, which may be one of the reasons why this formula behaves better for this case.

The calculation of a variety of return periods was conducted to assess the risks associated with the probability of occurrence of flooding episodes, based on extreme values analysis with a logarithm curve fit. Then, flood maps cartography was carried out considering the levels of wave runup at different return periods, as well as a validation storm and the topography of the area by using an adaptation of the bathtub approach. As the bathtub approach has multiple limitations, a reduction coefficient was empirically added to it to get a more realistic flood extension, by calibrating the flooded area with a past flooding episode, as the tilted bathtub approach.

Different IPCC scenarios were also implemented in the flood analysis to assess the sea-level rise impacts on wave runup events, which have presented a dramatic increase in the occurrence of flooding events, almost doubling it, as well as mildly increasing the overwash potential.

Although determining risk requires a well-detailed characterization of the occupation and values of the affected areas, the flood extensions serve as a crucial basis to implement adaptation to situations of flooding, as well as helping managers and stakeholders to take decisions. Despite the limitations of this work, this study has presented a simple, yet fair accurate, methodology to assess the flood risk in an area with high complexity and extreme vulnerability.

Bibliography

- Antena 3 Noticias. 2018. "El Campo de Fútbol de Garachico, Arrasado Por El Temporal: 'Es Un Solar de Asfalto.'" : 1–11.
- Baldock, T E. 2022. "Assessment and Optimisation of Runup Formulae for Beaches Fronted by Fringing Reefs Based on Physical Experiments." *Coastal Engineering* 176(June): 104163. <https://doi.org/10.1016/j.coastaleng.2022.104163>.
- Chris Leaman, & Dependabot. (2019). *chrisleaman/py-wave-runup: v0.1.4 (v0.1.4)*. Zenodo. <https://doi.org/10.5281/zenodo.2697004>
- Dodet, G. et al. 2018. "Wave Runup Over Steep Rocky Cliffs." *Journal of Geophysical Research: Oceans* 123(10): 7185–7205.
- Donnelly, Chantal. 2008. Doctoral Thesis *Coastal Overwash: Processes and Modelling*.
- Dottori, F., M. L.V. Martina, and R. Figueiredo. 2018. "A Methodology for Flood Susceptibility and Vulnerability Analysis in Complex Flood Scenarios." *Journal of Flood Risk Management* 11: S632–45.
- Ferreira, O. et al. 2018. "Storm-Induced Risk Assessment: Evaluation of Two Tools at the Regional and Hotspot Scale." *Coastal Engineering* 134(September 2017): 241–53.
- Ferreira, Óscar, Sunna Kupfer, and Susana Costas. 2021. "Implications of Sea-Level Rise for Overwash Enhancement at South Portugal." *Natural Hazards* 109(3): 2221–39. <https://doi.org/10.1007/s11069-021-04917-0>.
- Ferreira, Óscar, Theocharis A. Plomaritis, and Susana Costas. 2019. "Effectiveness Assessment of Risk Reduction Measures at Coastal Areas Using a Decision Support System: Findings from Emma Storm." *Science of the Total Environment* 657: 124–35.
- Galland, J.C. 1994. "Rubble Mound Breakwater Stability under Oblique Waves: And Experimental Study." 77(1977): 1061–74.
- Gomes da Silva, Paula, Giovanni Coco, Roland Garnier, and Antonio H.F. Klein. 2020. "On the Prediction of Runup, Setup and Swash on Beaches." *Earth-Science*

Reviews 204(October 2019): 103148.
<https://doi.org/10.1016/j.earscrev.2020.103148>.

Holman, R. A. 1986. "Extreme Value Statistics for Wave Run-up on a Natural Beach." *Coastal Engineering* 9(6): 527–44.

Howe, Daniel. 2016. "Bed Shear Stress Under Wave Runup on Steep Slopes."

Jiménez, José A. et al. 2015. "Resilience-Increasing Strategies for Coasts – Toolkit Coastal Hazard Assessment Module." (May): 123.

Kupfer, S., O. Ferreira, and S. Costas. 2020. "Assessment of Overwash-Induced Flooding at Two Beaches along the Southwest Algarve, Portugal." *Journal of Coastal Research* 95(sp1): 484–89.

McGranahan, Gordon, Deborah Balk, and Bridget Anderson. 2007. "The Rising Tide: Assessing the Risks of Climate Change and Human Settlements in Low Elevation Coastal Zones." *Environment and Urbanization* 19(1): 17–37.

Nielsen, P., and D. J. Hanslow. 1991. "Wave Runup Distributions on Natural Beaches." *J. Coastal Research* 7(4): 1139–52.

Plomaritis, Theocharis A., Óscar Ferreira, and Susana Costas. 2018. "Regional Assessment of Storm Related Overwash and Breaching Hazards on Coastal Barriers." *Coastal Engineering* 134(August): 124–33.

Plomaritis, Theocharis A, Susana Costas, and Oscar Ferreira. 2018. "Use of a Bayesian Network for Coastal Hazards, Impact and Disaster Risk." *Coastal Engineering* 134(February 2017): 134–47.

Poate, Timothy G., Robert T. McCall, and Gerd Masselink. 2016. "A New Parameterisation for Runup on Gravel Beaches." *Coastal Engineering* 117: 176–90. <http://dx.doi.org/10.1016/j.coastaleng.2016.08.003>.

Power, Hannah E. et al. 2019. "Prediction of Wave Runup on Beaches Using Gene-Expression Programming and Empirical Relationships." *Coastal Engineering* 144(November 2018): 47–61. <https://doi.org/10.1016/j.coastaleng.2018.10.006>.

Romero Ruiz, Carmen, and Esther Beltrán Yanes. 2015. "El Impacto de Las Coladas de 1706 En La Ciudad de Garachico. (Tenerife, Islas Canarias, España)."

- Investigaciones Geográficas* (63): 99.
- Ruggiero, Peter et al. 1991. "Of Coastal Properties Backing Beaches." 17(2): 407–19.
- Sallenger, Jr. 2000. "Storm Impact Scale for Barrier Islands." *Journal of Coastal Research* 16(3): 890–95.
- Stockdon, Hilary F., Rob A. Holman, Peter A. Howd, and Asbury H. Sallenger. 2006. "Empirical Parameterization of Setup, Swash, and Runup." *Coastal Engineering* 53(7): 573–88.
- The EurOtop team. 2018. "Eurotop 2018; Manual on Wave Overtopping of Sea Defences and Related Structures. An Overtopping Manual Largely Based on European Research, but for Worldwide Application." : 320. www.overtopping-manual.com.
- Villanueva Guimerans, Perfecto, and Antonio Ruiz Cañavate. 1994. "Oceanographic Characteristics of the Canary Islands." *International Hydrographic Review* LXXI(1)(March): 67–78.
- Vousdoukas, Michalis I. et al. 2016. "Developments in Large-Scale Coastal Flood Hazard Mapping." *Natural Hazards and Earth System Sciences* 16(8): 1841–53.
- Vousdoukas, Michalis Ioannis, Dagmara Wziatek, and Luis Pedro Almeida. 2012. "Coastal Vulnerability Assessment Based on Video Wave Run-up Observations at a Mesotidal, Steep-Sloped Beach." *Ocean Dynamics* 62(1): 123–37.
- Ward, P. J., H. De Moel, and J. C.J.H. Aerts. 2011. "How Are Flood Risk Estimates Affected by the Choice of Return-Periods?" *Natural Hazards and Earth System Science* 11(12): 3181–95.
- Wolters, Guido, and Marcel Van Gent. 2011. "Oblique Wave Attack on Cube and Rock Armoured Rubble Mound Breakwaters." *Coastal Engineering Proceedings* 1(32): 34.
- Yanes, A, M^a V Marzol, and C Romero. 2006. "Characterization of Sea Storms along the Coast of Tenerife , the Canary Islands." *Journal of Coastal Research* (48): 124–28.

Appendix

Power's formula for wave runup:

$$\begin{aligned}
 R_2 = H_s \times & \left((x_2 + \left(\left(\frac{x_3 \times 3}{e^{-5}} \right) \times ((3 \times x_3) \times x_3) \right) \right) \\
 & + \left(\left((x_1 + x_3) - 2 \right) - (x_3 - x_2) \right) + ((x_2 - x_1) - x_3) \\
 & + \left(\left((x_3^{x_1}) - \left(x_3^{\frac{1}{3}} \right) \right) - \left((e^{x_2})^{(x_1 \times 3)} \right) \right) \\
 & + \sqrt{\left((x_3 + x_1) - x_2 \right) - (x_2 + \log_{10} x_3)} \\
 & + \left(\left(\frac{(x_2^2)}{x_1 \left(\frac{1}{3} \right)} \right) + \log(2) - \left(\frac{1}{1 + \exp^{-(x_2 + x_3)}} \right) \right) + (x_1^{x_3}) \\
 & + \exp^{-\left(\left(\left(\frac{x_3}{x_1} \right)^{\exp^4} \right) + ((\exp^{x_3})^3) \right)^2} + \exp^{\left(\log(x_2 - x_3) - \log(\exp - ((-1 + x_1)^2)) \right)} \\
 & + \left(\left(\sqrt{4} \times \left(\left(\left(\frac{x_3}{x_2} \right) - x_2 \right) - (0 - x_1) \right) \right) \right)^2 \\
 & + \left(2 \times \left(\left((-5 \times x_3) + x_1 \right) \times (2 - x_3) \right) - 2 \right) \\
 & + \left(\sqrt{4} \times \left(\left(\left(\frac{x_3}{x_2} \right) - x_2 \right) - (0 - x_1) \right) \right)^2 \\
 & + \left(\left((-5 + x_1) - x_2 \right) \times (x_2 - x_3) \right) \times \left((x_1 - x_2) - (-4^{-5}) \right) \\
 & + \left(\exp^{-\left((x_2 + (-5 - x_1))^2 \right)} + \left((x_2 + 5) \times (x_3^2) \right) \right) \\
 & + \sqrt{1 / \left(1 + \exp^{-\left(\left(\exp^{x_1} - \exp^{-(x_3 + x_3)^2} \right) + \left((x_1^{x_3}) - (x_3 \times 4) \right) \right)} \right)} \\
 & + \left(\exp^{-\left(\left(\left(\left(\sqrt{x_3} \times 4 \right) + \left(\frac{1}{1 + \exp^{-(x_2 + 2)}} \right) \right) \right)^2 + x_1^2 \right)^3} \right) \quad (\text{Power, et al. 2019})
 \end{aligned}$$

Footage of past flooding events at Garachico:

<https://www.youtube.com/watch?v=19VEQpQgMY4>

<https://www.youtube.com/watch?v=zCikX80oZQ>

<https://www.youtube.com/watch?v=LRqXSaeiKol&t=30s>

<https://www.youtube.com/watch?v=c3BuvlYg0JA>

<https://www.youtube.com/watch?v=7hoG4-8MpWA>

<https://www.youtube.com/shorts/ia68U5QOIcc>